Pertanika J. Sci. & Technol. 34 (2): 823 - 844 (2026)

PERTANIKA JOURNALS

SCIENCE & TECHNOLOGY

Journal homepage: http://www.pertanika.upm.edu.my/

Green Synthesis of Carbon Dots from Empty Fruit Bunch Using Hydrothermal for Tetracycline Removal

Wan Nuraishah Wan Ishak[1], Ying Pei Lim[1]*, Huey Ling Tan[1], Noor Fitrah Abu Bakar[1], Ng Law Yong[2,3], and Chun Yang Yin[4]

[1]School of Chemical Engineering, College of Engineering, Universiti Teknologi MARA, 40450 Shah Alam, Selangor, Malaysia

[2]Department of Chemical Engineering, Lee Kong Chian Faculty of Engineering and Science, Universiti Tunku Abdul Rahman, Jalan Sungai Long, Bandar Sungai Long, 43000 Kajang, Selangor, Malaysia

[3]Centre for Advanced and Sustainable Materials Research (CASMR), Universiti Tunku Abdul Rahman, Jalan Sungai Long, Bandar Sungai Long, 43000 Kajang, Selangor, Malaysia

[4]College of Engineering and Computer Science, VinUniversity, Vinhomes Ocean Park, Gia Lam, 10000 Hanoi, Vietnam

ABSTRACT

Tetracycline (TCs) residues in wastewater present serious environmental and health risks, necessitating the development of efficient and sustainable remediation strategies. This study reports the green synthesis of carbon dots (CDs) derived from oil palm empty fruit bunches (EFB) through a one-pot hydrothermal process, offering an eco-friendly alternative for antibiotic degradation. The synthesised CDs were characterised by SEM-EDX, TEM, UV-DRS, FTIR, and XRD analyses, confirming their structural and optical properties. Photocatalytic experiments were conducted under various conditions, including different catalyst dosages (0.5-2.5 g/L), initial TCs concentrations (5-25 ppm), and light sources (solar, visible, and UV). The CDs achieved a maximum degradation efficiency of 50.14% at 1 g/L dosage and 5 ppm TCs concentration under UV light. Moreover, the CDs demonstrated good stability and reusability across multiple cycles. Mechanistic analysis suggests that photocatalytic degradation primarily involves the generation of hydroxyl (•OH) and superoxide ($O_2•^-$) radicals. These findings highlight the potential of biomass-derived CDs as an efficient, sustainable, and reusable photocatalyst for antibiotic removal from wastewater.

Keywords: Antibiotic degradation, biomass valorisation, carbon nanomaterials, photocatalytic activity, sustainable wastewater treatment

ARTICLE INFO

Article history:
Received: 13 February 2025
Accepted: 06 June 2025
Published: 17 April 2026

DOI: https://doi.org/10.47836/pjst.34.2.10

E-mail addresses:
2022288228@student.uitm.edu.my (Wan Nuraishah Wan Ishak)
hueyling@uitm.edu.my (Huey Ling Tan)
fitrah@uitm.edu.my (Noor Fitrah Abu Bakar)
lyng@utar.edu.my (Law Yong Ng)
chunyang.y@vinuni.edu.vn (Chun Yang Yin)
yingpei@uitm.edu.my (Ying Pei Lim)
* Corresponding author

e-ISSN: 2231-8526

INTRODUCTION

Antibiotic contamination in water bodies has become a global environmental concern due to its role in promoting antimicrobial resistance (AMR), which the World Health Organisation (2021) has identified as a major public health threat of the 21st century. Among the various antibiotics, tetracyclines (TCs) are the second most widely used group after sulfonamides, with extensive applications in human healthcare, veterinary medicine, and aquaculture (Niu et al., 2013). The frequent use and poor metabolisation rates of TCs result in their continuous discharge into the environment, contributing to the development of antibiotic-resistant bacteria and genes. In Malaysia, for example, Thiang et al. (2021) reported the presence of 23 antibiotics, including a high detection frequency of TCs in aquaculture farms. Similar pollution has been recorded globally, from Europe to North America and Asia, highlighting its widespread environmental relevance. Therefore, the removal of TCs from wastewater is a pressing global necessity.

Conventional wastewater treatment methods, such as ozonation, enzymatic degradation, activated carbon adsorption, and chlorination, have shown limited effectiveness in completely removing persistent pharmaceutical pollutants (Abejón et al., 2015; Gopal et al., 2020; Saadati et al., 2016). As a result, advanced oxidation processes (AOPs), particularly photocatalysis, have garnered significant attention as sustainable and promising alternatives. Photocatalysis, a green AOP that utilises light energy to activate semiconductor materials that generate reactive oxygen species (ROS) capable of mineralising organic contaminants, offering an eco-friendly and efficient method for antibiotic degradation (Hak et al., 2020). In this study, carbon dots (CDs) were synthesised using empty fruit bunch (EFB), a lignocellulosic agricultural waste generated in large quantities during crude palm oil (CPO) production. EFB is a fibrous byproduct obtained after the removal of oil-rich fruits from fresh fruit bunches during the sterilisation and threshing steps in palm oil milling. According to Hasanudin et al. (2023), approximately 20-22 million tonnes of EFB are produced annually in Malaysia, making it one of the most abundant biomass wastes in the country. Due to its high cellulose and lignin content, EFB is a promising, renewable carbon source for the synthesis of nanomaterials. Utilising EFB not only adds value to agricultural waste but also supports circular bioeconomy initiatives and reduces the environmental burden associated with biomass disposal. This aligns with the findings of Hasanudin et al. (2023), who emphasised the underutilised potential of EFB in Malaysia's palm oil industry.

Among various photocatalysts, carbon dots (CDs) have recently attracted significant attention due to their unique optical properties, tunable band gaps (2.47-4.5 eV), abundant surface functionalities, and excellent electron transfer capabilities (Jumardin et al., 2021; Khairol Anuar et al., 2021; Sutanto et al., 2020). CDs possess numerous surface functional groups and exhibit a hybrid structure of amorphous and nanocrystalline domains (Liu et al., 2020). With sizes below 10 nm, CDs are considered highly promising nanomaterials

for environmental remediation due to their strong photoluminescence, good absorption properties, and environmentally benign nature (Akbar et al., 2021; Liu et al., 2020). Among carbon nanomaterials such as nanotubes, fullerenes, and graphene, CDs have shown promise in photocatalysis because of their tunable band gap and rich surface chemistry (Jamaludin et al., 2018). Several studies have reported the application of CDs derived from agricultural biomass such as rice husk, banana peel, and sugarcane bagasse for pollutant degradation (Liu et al., 2020). CDs synthesised from oil palm biomass, including EFB, have been reported. However, their specific application in the photocatalytic degradation of antibiotics such as tetracycline remains significantly underexplored.

Recently, CDs have emerged as versatile photocatalysts for wastewater treatment, demonstrating high efficiency in degrading organic pollutants and antibiotics. Notably, CDs achieved 96% and 98% degradation of methylene blue and Congo red, respectively (Sawalha et al., 2021). Furthermore, CDs possess the ability to be tailored via functionalisation for specific applications. For instance, Liu et al. (2020) reported the synthesis of magnetic polyethyleneimine-functionalised carbon quantum dots, incorporating CDs into magnetic nanomaterials, which achieved an impressive uranium removal efficiency of 88%. CDs also show promising performance in removing polycyclic aromatic hydrocarbons (PAHs) such as benzopyrene, with an adsorption efficiency of 93.9% with the use of 9mg fatty acid-coated magnetic nanoparticles at a temperature of 25 °C (Cui et al., 2021). Apart from dyes and PAHs, CDs can be combined with other photocatalysts to degrade antibiotics. For example, CDs with bismuth vanadate and tantalates achieved 89.3% and 87.1% removal of amoxicillin and ciprofloxacin, respectively (Abinaya et al., 2021; Bai et al., 2022; Mukherjee et al., 2021).

Despite their promising photocatalytic activity, critical knowledge gaps persist regarding the reusability and underlying mechanisms of CDs. While numerous studies highlight their efficacy, comprehensive investigations into this area remain limited. However, existing studies have rarely explored the photocatalytic mechanism, reusability, and radical interaction pathways of biomass-derived CDs in antibiotic degradation, particularly in the context of tetracycline. Bridging these gaps is essential for realising the full potential of CDs in practical wastewater treatment applications. CDs can be synthesised using two main methods, which are the top-down approach and the bottom-up approach (Liu et al., 2020). The chosen method significantly impacts CDs' characteristics, including surface functional groups, size, and photoluminescence properties (Khairol Anuar et al., 2021). Top-down methods (arc-discharge, laser ablation) offer precise size control but require expensive equipment, harsh conditions, and often yield low quantities. Bottom-up approaches (hydrothermal, microwave, pyrolysis) are simple, low-cost, and scalable, yet can suffer from broader size distributions and longer reaction times. Among these, hydrothermal synthesis, classified as a bottom-up method, is widely favoured due

to its simplicity, environmental friendliness, cost-efficiency, and feasibility for large-scale production (Liu et al., 2020).

This study aims to contribute to the advancement of green nanomaterials by utilising EFB, a major agricultural waste product in Malaysia and Southeast Asia, for the sustainable synthesis of CDs. This valorisation not only promotes environmental sustainability by mitigating EFB disposal issues but also introduces a novel, renewable photocatalyst for antibiotic removal. Specifically, this study synthesises CDs via a hydrothermal method using EFB as the carbon precursor, characterises their structural, optical, and morphological properties using TEM, XRD, UV-DRS, and FTIR, evaluates their photocatalytic performance for tetracycline degradation under different operational parameters, and investigates the underlying photocatalytic mechanism through reactive species trapping experiments. To our knowledge, this is the first study utilising hydrothermally synthesised CDs derived from EFB for the photocatalytic degradation of tetracycline, addressing a critical gap in antibiotic wastewater remediation using palm biomass.

MATERIALS AND METHODS

Material

Empty fruit bunches were sourced from a palm oil plantation located in Selangor, Malaysia. Tetracycline (TCs > 95%) antibiotics with the molecular formula of $C_{22}H_{24}N_2O_8$ were supplied by Merck Millipore. All chemicals were analytical grade and were used without further purification. Deionised (DI) water served as the solvent for solution preparation. UV lamps, Kintons KT6-UVC (2 units x 15 W) were procured from a local Malaysian supplier.

Synthesis of Carbon Dots

The EFB was subjected to a rigorous washing procedure with tap water to eliminate any adhering contaminants or debris. Subsequently, the EFB was spread out in a monolayer and exposed to direct sunlight until complete desiccation was achieved. The dried EFB was then mechanically grinded into smaller particles using a grinding machine. Finally, the grinded EFB was sieved through a mesh of 0.25 mm mesh to obtain a uniform particle size distribution. The sieved EFB particles were then mixed with deionised (DI) water. The synthesis of CDs was modified according to previous literature hydrothermal methods (Egorova et al., 2018; Mahat & Shamsudin, 2020), as illustrated in Figure 1. Briefly, 6 g of EFB powder was mixed with 150 mL of deionised (DI) water in a Teflon-lined autoclave reactor. The reactor was then subjected to hydrothermal treatment at 200 °C for 3 hours. Thereafter, the reactor was allowed to cool down overnight. The resultant brown solution

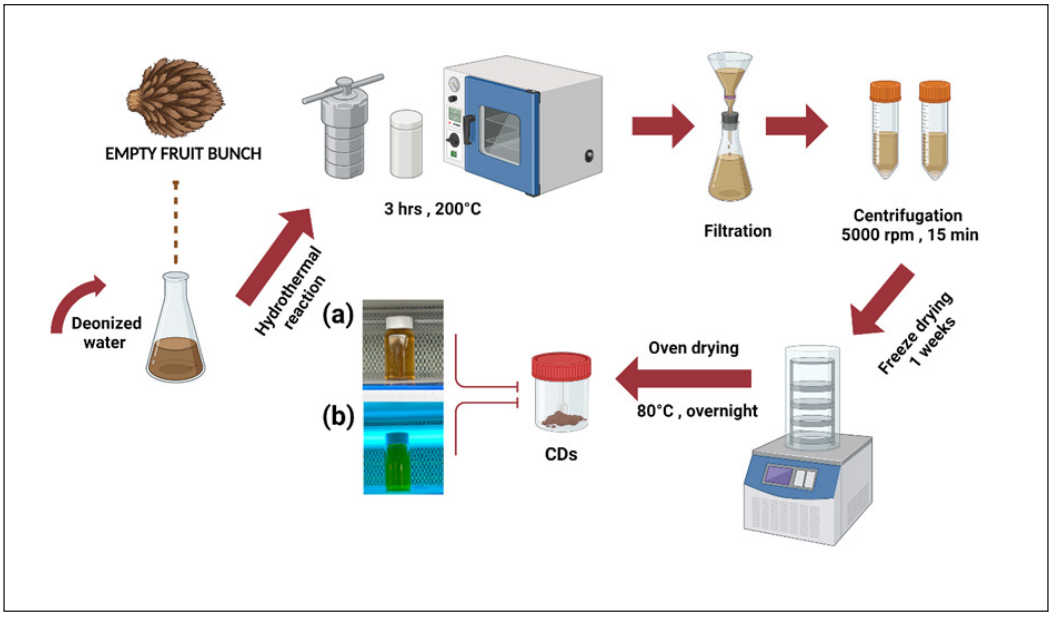

Figure 1. Synthesis route of carbon dots (CDs) derived from empty fruit bunch via the hydrothermal method. (a) CDs under daylight and (b) CDs under UV light

was centrifuged at 5000 rpm for 15 minutes to remove precipitates and larger particles. The final solution containing the synthesised CDs was then freeze-dried, followed by oven-drying at 80 °C, and stored for further characterisation.

Characterisation of Synthesised CDs

The functional group of the synthesised CDs was determined by Fourier Transform Infrared (FTIR) with a spectral range of 400 cm^{-1} to 4000 cm^{-1}. The crystalline structure of the photocatalyst was analysed using X-ray diffraction (Rigaku Ultima IV XRD) using monochromatised Cu Kα radiation of 40 kV and 30 mA with a scan rate of 8 min^{-1} between $2\theta = 10°$ to 90° with Cu Kα ($\lambda = 1.504$ Å). The morphology of the photocatalyst's structure was observed by Transmission Electron Microscope (TEM) using JEOL, 2100F at 200 kV. The CDs were dropped onto a copper grid and vacuum-dried for preparation before TEM characterisation. The elemental composition of CDs was determined by HITACHI scanning electron microscopy-energy-dispersive X-ray analysis (SEM-EDX) using 15 kV accelerating voltage. For SEM–EDX analysis of the carbon dots (CDs), each powder sample was mounted on a carbon-taped stub and sputter-coated with a thin layer of gold (~5 nm) using a Denton Desk V coater (Denton Vacuum, USA) to prevent charging effects. EDAX spectra were acquired on the freshly synthesised CDs, before any photocatalytic testing. The band gap was determined by Ultraviolet Diffuse Reflectance Spectroscopy (UV-DRS)

using a Shimadzu 3600. The diffuse reflectance spectroscopy was performed on the prepared sample using a PerkinElmer Lambda 750 UV-Vis/NIR spectrometer (Cary 300-800).

Photocatalytic Degradation of Tetracycline

The photocatalytic degradation test was conducted by mixing 1 g/L of synthesised CDs with 50 mL of 15 ppm TCs in a 100 mL Pyrex beaker over 180 minutes. Before light irradiation, the photocatalyst was stirred with tetracycline solution (15 ppm) in the dark for 30 minutes to establish adsorption-desorption equilibrium. This control step was conducted to assess the adsorption contribution and ensure any subsequent removal of tetracycline under light was due to photocatalytic degradation. Photocatalysis was then initiated by illuminating the solution with 2 units of 15 W UV lamps positioned 15 cm above the beaker. 5 mL of the solution was withdrawn from the beaker every 30 minutes by using a 0.22μm syringe filter. The concentration of TCs was determined from absorbance readings at 357nm using a Perkin Elmer UV-Vis/NIR Lamda 750. The photocatalytic degradation of TCs was repeated using different CDs dosages (0.5 g/L, 1.0 g/L, 1.5 g/L, 2.0 g/L, 2.5 g/L), TCs concentration (5 ppm, 10 ppm, 15 ppm, 20 ppm, 25 ppm) and source of light (solar light, visible light, UV light). For comparison with UV-induced degradation, additional photocatalytic tests were conducted under natural sunlight (10,000-30,000 lux intensity, clear sky, 12:00-2:00 PM) and visible light using an 80 W lamp with an emission peak at 400 nm. Control experiments were also conducted to evaluate photolysis and adsorption. For photolysis, the TCs solution was exposed to UV light without the addition of CDs, while for adsorption, the TCs solution was mixed with CDs and kept in the dark for 30 minutes. The percentage of TCs removal, E, was calculated using Equation 1 (Wu et al., 2020a), where C_i is the initial concentration of TCs antibiotics (ppm), and C_e is the equilibrium concentration of TCs antibiotics (ppm), respectively.

$$E(\%) = \frac{C_i - C_e}{C_i} \times 100\% \quad [1]$$

RESULTS AND DISCUSSION

Fourier Transform Infrared Spectroscopy (FT-IR)

Figure 2a illustrates the FTIR spectrum of the synthesised CDs. The broad peak observed at 3322 cm^{-1} corresponds to O–H stretching vibrations, indicating the presence of hydroxyl groups on the surface. A sharp peak at 1638 cm^{-1} is attributed to C=O stretching, suggesting carbonyl functional groups. A weaker peak appearing around 1538 cm^{-1} is assigned to N–H bending vibrations, indicating the incorporation of amine groups.

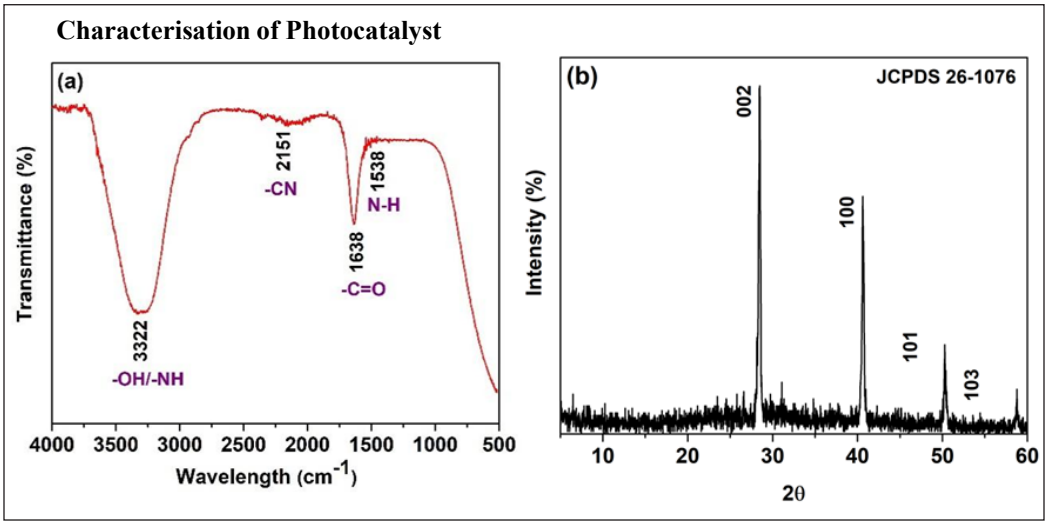

Figure 2. (a) FT-IR spectrum and (b) X-ray diffraction pattern of CDs

Additionally, a distinct peak at 2151 cm^{-1} is attributed to C≡N stretching, suggesting the presence of nitrogen-containing functionalities (Nair et al., 2020). The presence of these oxygen- and nitrogen-containing groups is typical for CDs synthesised via hydrothermal treatment and supports their hydrophilic nature and surface reactivity, as reported in previous studies (Ţucureanu et al., 2016).

X-ray Diffraction Analysis (XRD)

X-ray diffraction (XRD) analysis of the synthesised carbon dots (CDs), as depicted in Figure 2b, reveals a dominant peak at approximately 2θ = 28°, corresponding to the (002) plane of graphitic carbon, consistent with JCPDS No. 26-1076, indicating partial graphitisation. In addition to this primary peak, several distinct reflections are observed at around 2θ = 43°, 50.6°, and 58.8°, which can be assigned to the (100), (101), and (103) planes, respectively. These diffraction features suggest the presence of crystalline or semi-crystalline domains embedded within the carbon matrix. To validate the (002) assignment, Bragg's Law ($n\lambda = 2d \sin\theta$) was applied using Cu Kα radiation (λ = 0.15406 nm, n = 1, θ = 14°). The calculated interlayer spacing d = 0.319 nm, which agrees closely with the 0.32 nm lattice fringe spacing observed in HRTEM (Figure 3b). The absence of a broad hump commonly associated with amorphous carbon further supports the development of ordered structures during synthesis. These findings agree with previous studies on biomass-derived CDs synthesised via hydrothermal methods, which report similar XRD patterns indicative of polycrystalline characteristics and structural ordering (Jung et al., 2022; Mukherjee et al., 2021; N. Sharma et al., 2022).

Transmission Electron Microscopy (TEM) and Scanning Electron Microscope-energy Dispersive X-ray (SEM-EDX) Analysis

Figure 3a illustrates the morphology of the CDs from the TEM image. The synthesised CDs from EFB via the hydrothermal method were observed to have a spherical shape, consisting of a variety of sizes with slight aggregation, consistent with the findings stated by Xu et al. (2023) In Figure 3b, the lattice fringes of CDs are 0.32 nm, which corresponds well to the (002) plane of CDs in XRD analysis. This result is consistent with the work of Li et al. (2013). The size distribution of the CDs, measured to be less than 10 nm (Figure 3c), further corroborates their designation as nanomaterials, in agreement with previous studies (Liu et al., 2020). Table 1 presents the elemental composition of the synthesised CDs, determined by SEM-EDX. The values represent the average from multiple spot analyses to ensure accuracy and reduce operator bias. Carbon (30.4 wt%) and oxygen (46.1 wt%) were identified as the dominant elements, which is consistent with previous reports on carbon dots, where carbon and oxygen were similarly the predominant elements (Fawaz et al., 2023). The presence of minor elements such as K, Na, S, Ca, and Si can be ascribed to the inherent inorganic constituents of the biomass precursor. Potassium and sodium are biogenic elements inherently present in plant-derived biomass, typically absorbed from the soil during plant growth and retained during carbonisation or hydrothermal synthesis processes (Sahu & Sahoo, 2024). Oxygen is likely derived from oxygen-containing functional groups (e.g., –OH, –COOH, –C=O) introduced during the hydrothermal process. Sulphur detected in the CDs may be attributed to the natural sulphur content in the biomass, originating from intrinsic organic compounds and mineral uptake from soil and water, or retained within the ash content after hydrothermal treatment. Calcium and silicon are typically associated with residual mineral ash content within lignocellulosic biomass (Wang et al., 2022).

UV-Vis Diffuse Reflectance Spectroscopy (UV-DRS)

Analysis of the peaks in the optical absorption spectrum (Figure 4a) provides insights into the molecular transformations within the CDs. The sharp peak observed at 241 nm is attributed to the π-π^* transition in aromatic C-C and C=C bonds, while the peak at 287 nm corresponds to the n-π^* transition in C=O bonds (Mahat & Shamsudin, 2020). Additionally, a distinct tailing shape is observed in the wavelength range of 380 nm to 780 nm, corresponding to the visible light region. These findings are presented in Figure 4a, confirming the consistency of the synthesised CDs analysis with previous research (Abinaya et al., 2021). Moreover, Figure 1b shows the fluorescence behaviour of the CDs in solution under UV-light irradiation at a wavelength of 365 nm, where the CDs exhibited a green fluorescence. Conversely, the solution appeared as a light shade of brown under daylight, as shown in Figure 1a. This colouration agrees with the findings reported by Mahat and Shamsudin, (2020).

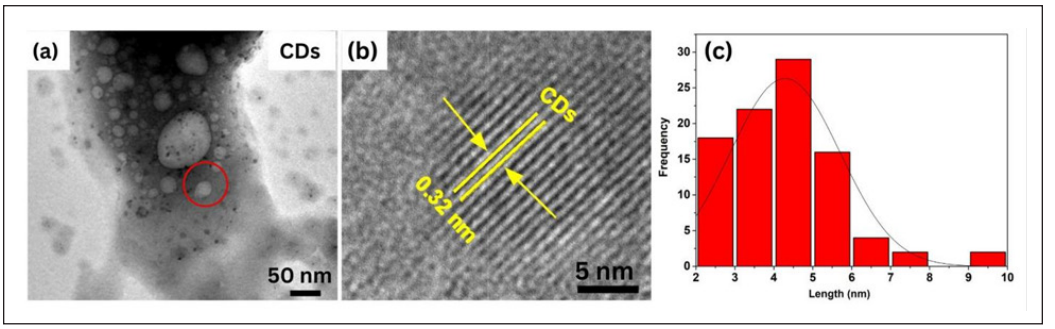

Figure 3. (a) TEM images; (b) HRTEM images; and (c) particle distribution of CDs

Table 1
Average elemental composition of CDs from multiple SEM-EDX spots

Element	C	O	K	Na	P	S	Ca	Cl	Si
Weight (%)	18.5	37.4	32.4	0.7	1.2	1.2	0.8	5.1	1.8
Atomic (%)	30.4	46.1	16.3	0.6	1.2	1.2	0.4	2.8	1.2

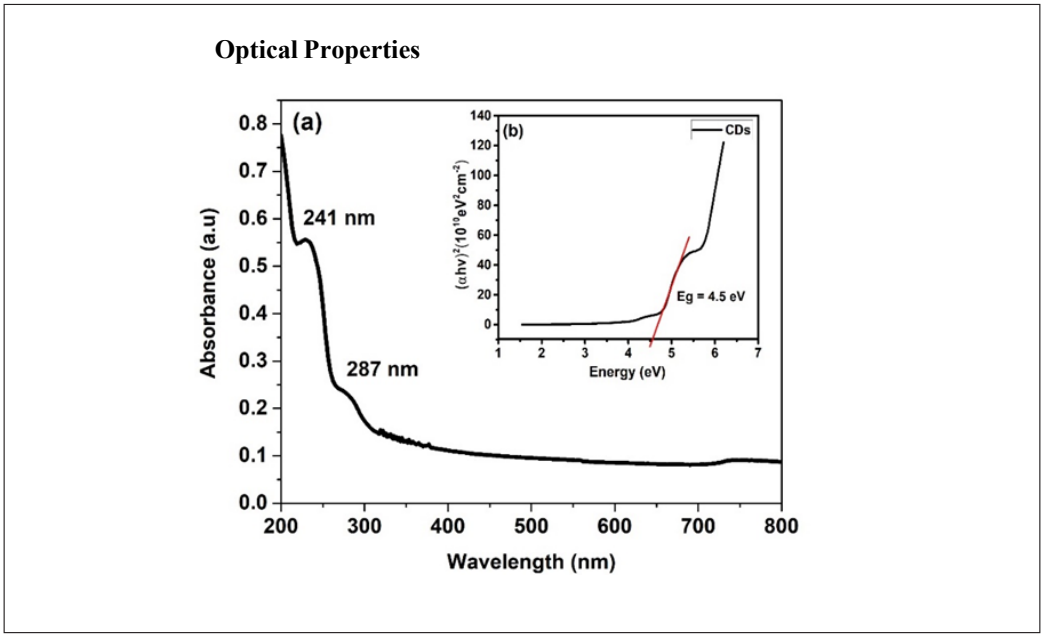

Figure 4. (a) UV-Vis diffuse reflectance of CDs and (b) Tauc plot of CDs for determination of the bandgap (inset)

The green fluorescence of CDs is primarily attributed to the presence of C=N bonds within their structure. These bonds are crucial as they influence the electronic structure, allowing CDs to emit green light when excited. This phenomenon is supported by previous studies showing that CDs with specific nitrogen concentrations exhibit significant photoluminescence due to C=N and C-N bonds (Hu et al., 2022). In addition, a wide band gap indicates that the material primarily responds to higher-energy photons, such as ultraviolet UV light, while a narrower band gap allows for the absorption of visible light. Therefore, understanding the band gap of a photocatalyst is vital for optimising its performance in applications such as pollutant degradation and wastewater treatment. The band gap of the photocatalyst was determined using Tauc's plot analysis as shown in Figure 4b. The plot of *hv* (photon energy) versus energy revealed a band gap value of 4.5 eV, indicating that the photocatalyst operates within the UV light range. This relatively large band gap suggests limited π-conjugation within the carbon core, likely influenced by quantum confinement effects and surface passivation. In contrast, most biomass-derived carbon dots typically exhibit band gaps in the range of 2.0-3.5 eV, depending on the source and synthesis conditions, e.g., CDs derived from chitosan or plant materials (Mintz et al., 2019). The higher band gap observed in our study may be attributed to specific factors, including the synthesis method and precursor composition, which could result in a more restricted π-conjugation and more prominent surface passivation. Additionally, quantum confinement effects due to the smaller particle size could further increase the band gap energy. As reported by Yu et al. (2018), both the carbon core and surface states contribute significantly to the optical behaviour of carbon dots, with surface states exhibiting a band gap of approximately 4.5 eV-narrower than the core's band gap (~5.0 eV). This supports our observation that optical transitions in the synthesised material are likely dominated by surface-state contributions. Similar findings have also been discussed by Mintz et al. (2019) and Zhou et al. (2018), who emphasised the role of surface functionalities in modulating the band structure and photophysical behaviour of carbon-based nanomaterials.

Effect of CD's Dosage

Figure 5a investigates the influence of photocatalyst (CDs) loading (0.5-2.5 g/L) on TCs degradation within 180 minutes for an initial TCs concentration of 15 ppm. An optimal CDs dosage of 1 g/L (red bar) is observed, corresponding to the highest TCs degradation efficiency (40.35%). This could be attributed to the increased availability of active sites on the catalyst surface at this concentration, facilitating a greater number of TCs molecules to undergo photocatalytic degradation into harmless byproducts like carbon dioxide and water. Our findings are aligned with previous reports who observed degradation rates of 83.5%, 86.2%, and 81.7% for CDs dosages of 0.5 g/L, 1 g/L, and 2 g/L, respectively (Saadati et al., 2016; Safari et al., 2015; Yan et al., 2015). It is also noteworthy that exceeding the

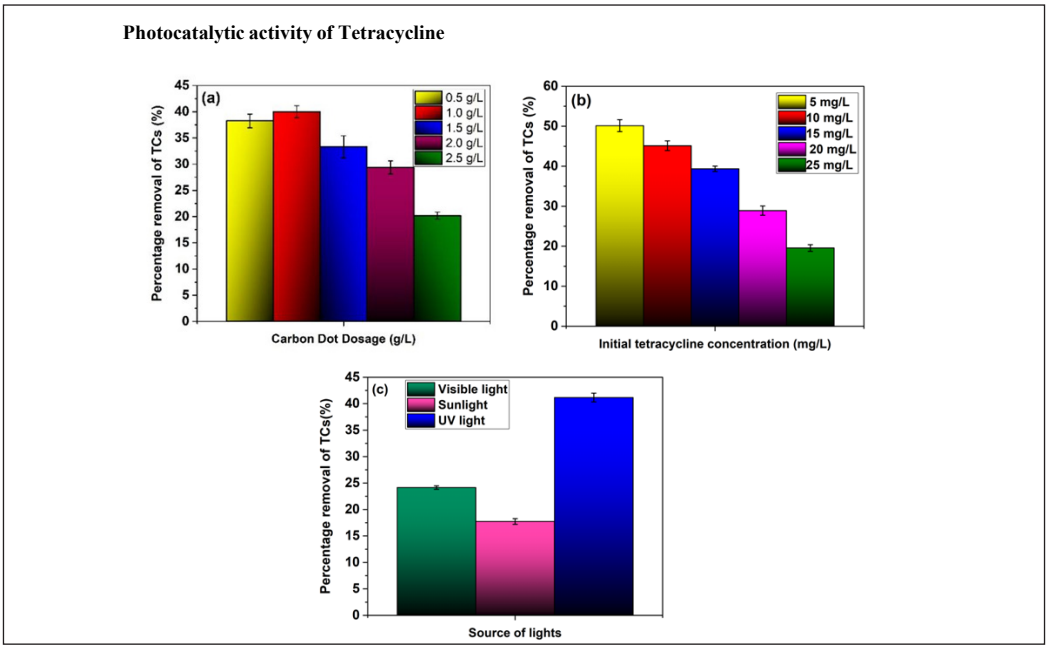

Figure 5. Percentage removal of TCs at different (a) dosages; (b) initial concentrations of tetracycline; and (c) sources of light

optimal CDs loading can hinder pollutant removal efficiency. A possible explanation for these decreases at higher CDs dosages could be the aggregation of photocatalysts, which restricts the accessibility of active sites and the generation of reactive species responsible for TCs degradation. Additionally, at high CDs loadings, the pollutant molecules might compete with excess CDs particles for available active sites on the catalyst surface, further hindering pollutant adsorption and degradation. Therefore, optimising catalyst loading and mitigating excessive aggregation are critical factors for maximising the photocatalytic performance in wastewater treatment applications. Similar observations were reported by those who identified an optimal dosage of 1.5 g/L, with degradation efficiency declining at higher loadings of 0.25-2.5 g/L (Azimi & Nezamzadeh-Ejhieh, 2015).

Effect of Concentration of TCs

Figure 5b depicts the TCs removal percentage by manipulating TCs concentration (5-25ppm) using 1 g/L CDs within 180 minutes. It was found that TCs removal efficiency was inverse of its concentration within the range of 5-25 ppm, with the highest removal efficiency recorded as 50.14 %. The correlation between the degradation pattern of TCs and its concentration could be attributed to the blocking effect of excessive TCs molecules,

which hinders the penetration of UV light in the solution (Wu et al., 2021b). In a similar work conducted by Saadati et al. (2016) the lowest TCs concentration (10 ppm) exhibited the highest degradation rate at 79.1 %. However, as TC concentration increased from 15 ppm to 20 ppm and 30 ppm, the percentage degradation of TCs decreased slightly. At lower TCs concentrations, the CDs did not experience surface saturation, thus enabling rapid photocatalytic production of superoxide and hydroxyl ions for pollutant degradation (Niu et al., 2013). Initial tetracycline concentrations (15-25 ppm) were selected based on previous laboratory-scale photocatalytic studies of antibiotic removal and to represent highly contaminated pharmaceutical effluent conditions. This range is commonly used in the literature to simulate realistic pollution scenarios and evaluate photocatalytic efficiency under such conditions.

Effect of Source of Light on the CDs

In the present work, UV-light, visible light and solar were selected to investigate the effect of the light source on the TCs removal (TCs concentration: 15 ppm, CDs dosage: 1 g/L). As illustrated in Figure 5c, the TC's degradation efficiency corresponding to the effect of light source followed: UV light (41.2%) > visible light > (24.15%) > sunlight (17.74%). This observation could be attributed to the band gap of the synthesised CDs (~4.5 eV), which primarily absorbs light in the UV region as shown in Figure 4 (inset). The relatively low photocatalytic degradation efficiency observed under UV irradiation may be attributed to the wide band gap (4.5 eV) of the synthesised carbon dots, which limits their light absorption to the UV range and may reduce the generation and separation efficiency of charge carriers. Additionally, surface-related recombination and the absence of co-catalysts or composite structures could also contribute to the limited activity. These findings are consistent with previous studies by Zhong et al. (2020) and M. Sharma et al. (2022), who also observed reduced photocatalytic degradation of sulfamethoxazole (SMX) and enrofloxacin (ENR) under visible light compared to UV light. Similarly, Khan et al. (2010) reported a significantly higher degradation efficiency (71.8%) under UV irradiation, compared to 40% under visible light. Interestingly, although sunlight contains both UV and visible light components, its degradation efficiency was lower than that under visible light alone. This counterintuitive result may be due to several contributing factors. Firstly, solar irradiance is naturally variable and dependent on atmospheric and geographic conditions, potentially causing fluctuations in light intensity during the reaction period (Chong et al., 2010).

Secondly, the proportion of UV photons in sunlight during the early afternoon (12:00-2:00 PM) could have been relatively low, with the spectral distribution shifting more toward longer wavelengths. In contrast, the visible light source used in this study

emitted strongly at 400 nm, providing a more consistent and effective excitation of the CDs. Thirdly, outdoor exposure under sunlight may introduce scattering, reflective losses, or elevated solution temperatures, all of which can negatively affect photocatalytic activity through reduced photon flux or enhanced recombination of charge carriers (Pelaez et al., 2012). Furthermore, CDs demonstrated some activity under visible light irradiation, possibly due to surface states or defect sites that can trap visible light photons (Akbar et al., 2021). This facilitates electron-hole pair generation despite the larger band gap. These defects can introduce intermediate energy levels within the band gap, reducing the energy required for electron excitation and enabling visible light absorption (Liu et al., 2020).

The reusability and stability of the synthesised carbon dots (CDs) were evaluated for their efficacy in tetracycline degradation through five consecutive cycles under identical reaction conditions (5 ppm tetracycline, 1 g/L CDs, 180 minutes irradiation time). Following each cycle, the reaction media were centrifuged to recover the CDs. The recovered CDs were then thoroughly washed with a 1:3 ethanol/water mixture (w/w or v/v) and oven-dried at 80 °C overnight (Mukherjee et al., 2021). As shown in Figure 6a, the tetracycline degradation efficiency exhibited a minimal decrease from 50.08% in the initial cycle to 44.01% after the fifth recycling cycle. Furthermore, X-ray diffraction (XRD) analysis was performed on the CDs before and after the five-cycle experiment to assess the reuse of the CDs' structural integrity. The XRD results demonstrated no significant changes in the crystalline structure of the CDs, indicating their high chemical stability throughout the degradation process (Figure 6c). Various scavenging experiments were conducted following the established protocol by previous literature (Niu et al., 2013; Trenczek-Zajac et al., 2022; Wu et al., 2020a) to elucidate the dominant reactive species involved in the photocatalytic degradation of tetracycline using CDs under UV light irradiation. The employed scavengers included ethylenediamine tetraacetic acid disodium salt (EDTA-2Na) for h^+, silver nitrate ($AgNO_3$) for e^-, p-benzoquinone (p-BQ) for $\bullet O_2^-$, and tert-butanol (BuOH) for •OH radicals. As shown in Figure 6b, the introduction of EDTA-2Na and $AgNO_3$ did not significantly affect tetracycline degradation. Conversely, the inclusion of BuOH and PBQ as scavengers for •OH and $\bullet O_2^-$ radicals, respectively, significantly suppressed tetracycline degradation by 38.56% and 46.73%, respectively. These findings strongly suggest that •OH and $\bullet O_2^-$ radicals play the most critical roles in tetracycline degradation mediated by the CDs as shown in Figure 7. Generally, the effectiveness of photocatalytic degradation relies on the generation of ROS, which is contingent upon the photocatalyst's ability to suppress exciton recombination. This suppression enabled the excitons to undergo alternate transitions, thereby facilitating the production of ROS. Here, the CDs photocatalyst absorbs UV light of energy greater than its bandgap, inducing photoexcitation. This process promotes the transition of electrons from the valence band to the conduction band, generating electron-hole pairs (e^-/h^+) within the CDs. The electrons in the conduction band can interact with

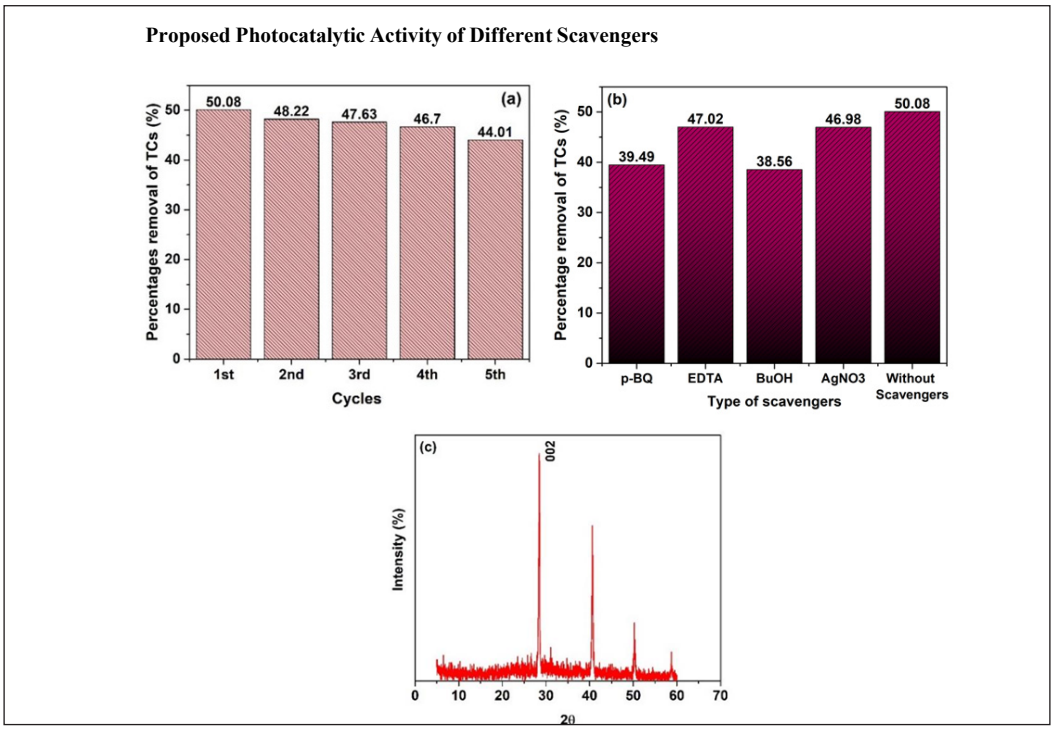

Figure 6. (a) Reusability of CDs up to five cycles; (b) scavenger test; and (c) XRD patterns of recycled photocatalyst

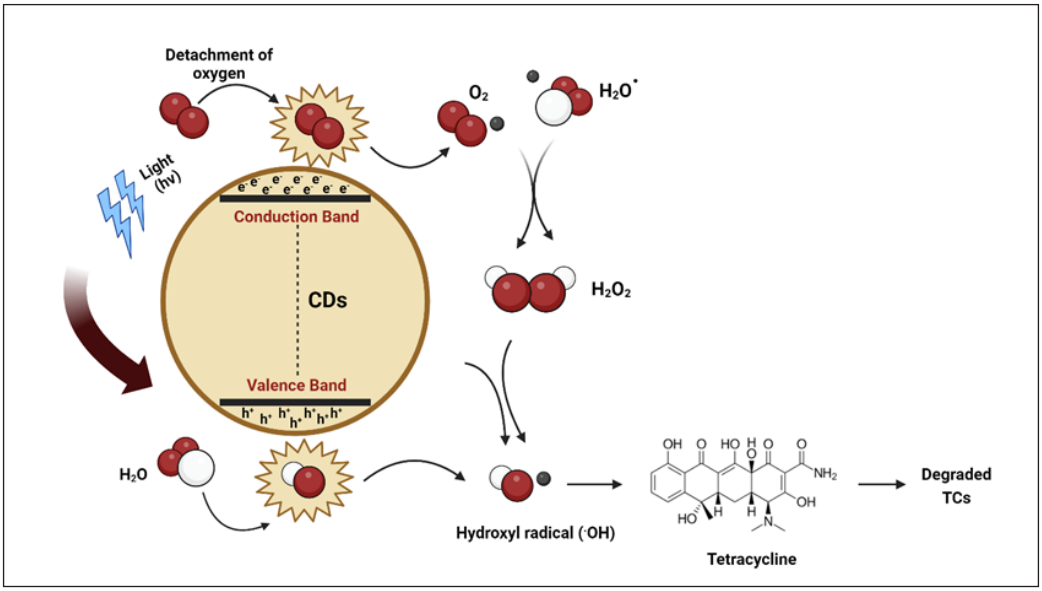

Figure 7. Proposed mechanism of degradation TCs by CDs

Table 2
The kinetic parameters at different concentrations of TCs degradation

Initial Concentration (mgL^{-1})	Reaction Rate, k (min^{-1})
5	0.0031
10	0.0028
15	0.0021
20	0.0014
25	0.01

oxygen (O_2) molecules to form superoxide radicals (O_2•-). Conversely, the holes in the valence band can react with water (H_2O) molecules to produce hydroxyl radicals (•OH) and hydrogen peroxide (H_2O_2). Notably, hydrogen peroxide (H_2O_2) can further decompose to generate additional hydroxyl radicals (•OH). The hydroxyl radicals (•OH), being highly reactive, attack the tetracycline (TCs) molecules, breaking them down into smaller, less harmful molecules. This phenomenon leads to the degradation of TCs into simpler, environmentally benign compounds, ultimately reducing its presence as a pollutant.

Kinetic study for the Photodegradation of TCs

The photodecomposition of TCs was further analysed using a pseudo-first-order kinetic model. The natural logarithm (ln) of the initial concentration of TCs (C_o) and the concentration remaining after a specific irradiation time (C_t) was plotted against irradiation time. The rate constant (k), representing the pseudo-first-order reaction rate coefficient, was then obtained from the slope of the resulting linear plot, and the data were depicted in Table 2. This approach provides an apparent first-order rate constant based on the straight slope of the ln (C_o/C_t) versus time relationship. Following the Langmuir-Hinshelwood (LH) kinetic model, the initial degradation rate (r_o) can be expressed by the Equation 2, 3, and 4:

$$-(\ln C - \ln C_o) = kt \quad [2]$$

$$r_o = -\frac{dC}{dt} = \frac{K_R K_{LH} C_o}{1 + K_{LH} C_o} = k_{app} C_o \quad [3]$$

$$\frac{1}{k_{app}} = \frac{1}{K_R K_{LH}} + \frac{C_o}{K_R} \quad [4]$$

where kr is the pseudo-first order Langmuir-Hinshelwood type rate coefficient, and k_{LH} is a pseudo-equilibrium constant related to monolayer adsorption on the catalyst surface (Equations 2 , 3, and 4). Our investigation into the normalised concentration versus 1/kapp plot suggests a two-step photodecomposition mechanism for TCs. The first step involves pollutant adsorption onto the active sites of CDs, followed by photochemical degradation consistent with the Langmuir-Hinshelwood (LH) kinetic model. The Langmuir-type correlation observed between the initial degradation rate and concentration strongly supports the occurrence of adsorption during the photocatalytic reaction. The Langmuir-type correlation observed between the initial degradation rate and concentration further supports this adsorption-controlled mechanism. Although the photocatalytic reaction takes place in a suspended system, the kinetic behaviour and adsorption parameters are consistent with the LH model, indicating that the degradation of tetracycline proceeds predominantly through surface-mediated mechanisms rather than bulk-phase reactions. Notably, the calculated reaction rate constant (k_r = 0.01654 mg L^{-1} min^{-1}) and the relatively high adsorption equilibrium constant, k_{LH} (1.7653 mg L^{-1}), indicate a strong interaction between TCs and the catalyst surface shown in Figure 8. These findings align with Syahin et al. (2019), who reported similar behaviour in the photocatalytic degradation of phenol. A comparative analysis presented in Table 3 reveals that the carbon dot photocatalyst synthesised in this study exhibited superior photocatalytic degradation of tetracycline compared to those reported in previous literature. These findings underscore the promising potential of the synthesised carbon dots in combating antibiotic contaminants present in water.

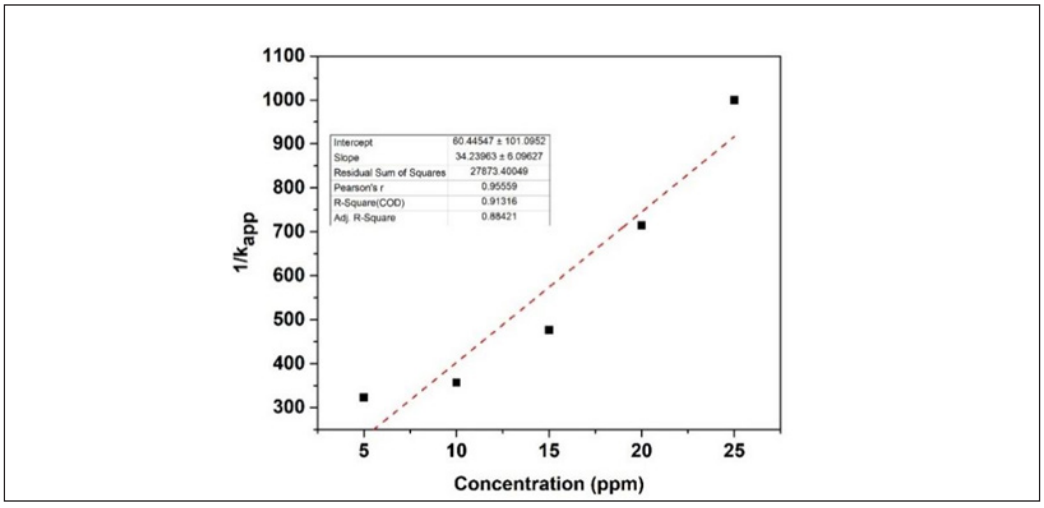

Figure 8. The relationship between $1/k_{app}$ and the initial concentration of TCs

Table 3
Comparison of previous literature on CDs based photocatalysts for photodegradation

Photocatalyst	Morphology	Source of Light	Degradation Efficiency	Fluorescence	References
Carbon dots	Spherical	Natural Sunlight	43 %, 10 hr for removal of methylene blue	Blue emission	(Jusuf et al., 2018)
Polymer-modified GQDs	Spherical	300 W, Xe lamp	45 %, 100 min for removal of methylene blue	Green emission	(Fan et al., 2016)
GQDs	Spherical	Natural Sunlight	45 %, 100 min for removal of methylene blue	-	(Kumar et al., 2017)
Carbon dots	-	Visible light	42.8 %, 8 days	Blue emission	(Liu et al., 2021)
$Bi_2O_2CO_3$/ NCQDs	Spherical	Near-infrared light	35 %, 360 min for removal of ciprofloxacin	-	(Hu et al., 2021)
Carbon dots	Spherical	UVB light	9.48 %, 60 min for decolourisation of the organic compound	-	(Ayu et al., 2023)
Carbon dots	-	Stimulated solar light	47 %, 4 hr for removal of antibiotics	Blue emission	(Louros et al., 2021)
Carbon dots	Spherical	UV light	50.14 %, 180 min for removal of tetracycline	Green emission	(Syahin et al., 2019)

CONCLUSION

In conclusion, this study successfully demonstrated the synthesis of carbon dots (CDs) from empty fruit bunch (EFB) waste via a simple one-pot hydrothermal method. The EFB-derived CDs exhibited efficient photocatalytic activity for tetracycline (TCs) degradation in wastewater treatment. Optimal TCs removal was achieved at a CDs dosage of 1 g/L and a TCs concentration of 5 ppm under UV light irradiation. Furthermore, preliminary studies indicate that the CDs exhibit good reusability and recyclability, suggesting their potential for long-term application in wastewater treatment. The photocatalytic mechanism primarily involves the generation of hydroxyl (•OH) and superoxide ($\bullet O_2$-) radicals under light irradiation, leading to the oxidation and mineralisation of TCs molecules. These findings highlight the potential of EFB as a sustainable precursor for photocatalyst production, contribute significantly to the field of environmental remediation and waste valorisation, offering a sustainable solution for both agricultural waste management and

water treatment. Future research efforts could focus on optimising the synthesis conditions to further enhance photocatalytic activity and explore the feasibility of immobilising CDs on suitable supports for practical wastewater treatment applications.

ACKNOWLEDGEMENT

This work was financially supported by the My RA (GPM/033/2022). The authors also extend their gratitude to the College of Engineering at Universiti Teknologi, MARA for their assistance in completing the research project.

LIST OF ABBREVIATIONS

AMR	:	Antimicrobial resistance
AOPs	:	Advanced oxidation processes
CDs	:	Carbon dots
CPO	:	Crude palm oil
DI	:	Deionised
EFB	:	Empty fruit bunch
FTIR	:	Fourier transform infrared spectroscopy
HRTEM	:	High resolution transmission electron microscopy
LH	:	Langmuir-Hinshelwood
PAHs	:	Polycyclic Aromatic Hydrocarbons
PL	:	Photoluminescence
ROS	:	Reactive oxygen species
SEM	:	Scanning electron microscopy
SEM-EDX	:	Scanning electron microscopy-energy dispersive X-ray
TEM	:	Transmission electron microscopy
TC	:	Tetracycline
TCs	:	Tetracyclines
UV	:	Ultraviolet
UV-DRS	:	Ultraviolet diffuse reflectance spectroscopy
UV–Vis	:	Ultraviolet-visible spectroscopy
XRD	:	X-ray diffraction
h^+	:	Hole
e^-	:	Electron
•OH	:	Hydroxyl radical
$O_2•^-$	:	Superoxide radical
H_2O_2	:	Hydrogen peroxide
EDTA-2Na	:	Ethylenediaminetetraacetic acid disodium salt
$AgNO_3$	:	Silver Nitrate
PBQ / p-BQ	:	p-Benzoquinone
BuOH	:	tert-Butanol

REFERENCES

Abejón, R., De Cazes, M., Belleville, M. P., & Sanchez-Marcano, J. (2015). Large-scale enzymatic membrane reactors for tetracycline degradation in WWTP effluents. *Water Research, 73*, 118-131.https://doi.org/10.1016/j.watres.2015.01.012

Abinaya, K., Rajkishore, S. K., Lakshmanan, A., Anandham, R., Dhananchezhiyan, P., & Praghadeesh, M. (2021). Synthesis and characterisation of carbon dots from coconut shell by optimising the hydrothermal carbonisation process. *Journal of Applied and Natural Science, 13*(4), 1151-1157.https://doi.org/10.31018/jans.v13i4.2916

Akbar, K., Moretti, E., & Vomiero, A. (2021). Carbon dots for photocatalytic degradation of aqueous pollutants: Recent advancements. *Advanced Optical Materials, 9*(17), Article 2100532.https://doi.org/10.1002/adom.202100532

Ayu, D. G., Gea, S., Andriayani, N., Telaumbanua, D. J., Piliang, A. F. R., Harahap, M., Yen, Z., Goei, R., & Tok, A. I. Y. (2023). Photocatalytic degradation of methylene blue using N-doped ZnO/carbon dot (N-ZnO/CD) nanocomposites derived from organic soybean. *ACS Omega, 8*(17), 14965-14984.https://doi.org/10.1021/acsomega.2c07546

Azimi, S., & Nezamzadeh-Ejhieh, A. (2015). Enhanced activity of clinoptilolite-supported hybridised PbS–CdS semiconductors for the photocatalytic degradation of a mixture of tetracycline and cephalexin aqueous solution. *Journal of Molecular Catalysis A: Chemical, 408*, 152-160.https://doi.org/10.1016/j.molcata.2015.07.017

Bai, X., Chen, W., Wang, B., Sun, T., Wu, B., & Wang, Y. (2022). Photocatalytic degradation of some typical antibiotics: Recent advances and future outlooks. *International Journal of Molecular Sciences, 23*(15), Article 8130.https://doi.org/10.3390/ijms23158130

Chong, M. N., Jin, B., Chow, C. W. K., & Saint, C. (2010). Recent developments in photocatalytic water treatment technology: A review. *Water Research, 44*(10), 2997-3027.https://doi.org/10.1016/j.watres.2010.02.039

Cui, L., Ren, X., Sun, M., Liu, H., & Xia, L. (2021). Carbon dots: Synthesis, properties and applications. *Nanomaterials, 11*(12), Article 3419. https://doi.org/10.3390/nano11123419

Egorova, M. N., Tomskaya, A. E., Kapitonov, A. N., Alekseev, A. A., & Smagulova, S. A. (2018). Hydrothermal synthesis of luminescent carbon dots from glucose and birch bark soot. *Journal of Structural Chemistry, 59*(4), 780-785. https://doi.org/10.1134/S0022476618040054

Fan, J., Li, D., & Wang, X. (2016). Effect of modified graphene quantum dots on photocatalytic degradation property. *Diamond and Related Materials, 69*, 81-85. https://doi.org/10.1016/j.diamond.2016.07.008

Fawaz, W., Hasian, J., & Alghoraibi, I. (2023). Synthesis and physicochemical characterisation of carbon quantum dots produced from folic acid. *Scientific Reports, 13*(1), Article 46084. https://doi.org/10.1038/s41598-023-46084-1

Gopal, G., Alex, S. A., Chandrasekaran, N., & Mukherjee, A. (2020). A review on tetracycline removal from aqueous systems by advanced treatment techniques. *RSC Advances, 10*(45), 27081-27095.https://doi.org/10.1039/D0RA04264A

Hak, C. H., Leong, K. H., Chin, Y. H., Saravanan, P., Tan, S. T., Chong, W. C., & Sim, L. C. (2020). Water hyacinth derived carbon quantum dots and g-C_3N_4 composites for sunlight driven photodegradation of 2,4-dichlorophenol. *SN Applied Sciences, 2*(6), Article 2840.https://doi.org/10.1007/s42452-020-2840-y

Hasanudin, Asri, W. R., Muthiarani, T. E., Bahrain, D., & Hadiah, F. (2023). Esterification of free fatty acid from sludge palm oil using zeolite sulfonated carbon from sugar cane catalysts. *Journal of Oil Palm Research, 35*(2), 268-280. https://doi.org/10.21894/jopr.2022.0051

Hu, C., Wang, K.-H., Chen, Y.-Y., Maniwa, M., Lin, K.-Y. A., Kawai, T., & Chen, W. (2022). Detection of Fe^{3+} and Hg^{2+} ions through photoluminescence quenching of carbon dots derived from urea and bitter tea oil residue. *Spectrochimica Acta Part A: Molecular and Biomolecular Spectroscopy, 272*, 120963. https://doi.org/10.1016/j.saa.2022.120963

Hu, X., Zhao, H., Liang, Y., Chen, F., Li, J., & Chen, R. (2021). Broad-spectrum response NCQDs/$Bi_2O_2CO_3$ heterojunction nanosheets for ciprofloxacin photodegradation: Unravelling the unique roles of NCQDs upon different light irradiation. *Chemosphere, 264*, 128434.https://doi.org/10.1016/j.chemosphere.2020.128434

Jamaludin, N., Rashid, S. A., & Tan, T. (2018). Natural biomass as carbon sources for the synthesis of photoluminescent carbon dots. In *Synthesis, technology and applications of carbon nanomaterials* (pp. 109-134). Elsevier. https://doi.org/10.1016/B978-0-12-815757-2.00005-X

Jumardin, J., Maddu, A., Santoso, K., & Isnaeni, I. (2021). Synthesis of carbon dots (CDs) and determination of optical gap energy with Tauc plot method. *Jambura Physics Journal, 3*(2), 73-86. https://doi.org/10.34312/jpj.v3i2.11235

Jung, H., Sapner, V. S., Adhikari, A., Sathe, B. R., & Patel, R. (2022). Recent progress on carbon quantum dots based photocatalysis. *Frontiers in Chemistry, 10*, Article 881495. https://doi.org/10.3389/fchem.2022.881495

Jusuf, B. N., Sambudi, N. S., Isnaeni, & Samsuri, S. (2018). Microwave-assisted synthesis of carbon dots from eggshell membrane ashes using sodium hydroxide and their usage for degradation of methylene blue. *Journal of Environmental Chemical Engineering, 6*(6), 7426-7433. https://doi.org/10.1016/j.jece.2018.10.032

Khairol Anuar, N. K., Tan, H. L., Lim, Y. P., So'aib, M. S., & Abu Bakar, N. F. (2021). A review on multifunctional carbon dots synthesised from biomass waste: Design/fabrication, characterisation and applications. *Frontiers in Energy Research, 9*, Article 626549.https://doi.org/10.3389/fenrg.2021.626549

Khan, M. H., Bae, H., & Jung, J. Y. (2010). Tetracycline degradation by ozonation in the aqueous phase: Proposed degradation intermediates and pathway. *Journal of Hazardous Materials, 181*(1-3), 659-665. https://doi.org/10.1016/j.jhazmat.2010.05.063

Kumar, S., Ojha, A. K., Ahmed, B., Kumar, A., Das, J., & Materny, A. (2017). Tunable (violet to green) emission by high-yield graphene quantum dots and exploiting its unique properties towards sunlight-driven photocatalysis and supercapacitor electrode materials. *Materials Today Communications, 11*, 76-86. https://doi.org/10.1016/j.mtcomm.2017.02.009

Li, Y., Zhang, B. P., Zhao, J. X., Ge, Z. H., Zhao, X. K., & Zou, L. (2013). ZnO/carbon quantum dots heterostructure with enhanced photocatalytic properties. *Applied Surface Science, 279*, 367-373.https://doi.org/10.1016/j.apsusc.2013.04.114

Liu, J., Li, R., & Yang, B. (2020). Carbon dots: A new type of carbon-based nanomaterial with wide applications. *ACS Central Science, 6*(12), 2179-2195. https://doi.org/10.1021/acscentsci.0c01306

Liu, Y. Y., Yu, N. Y., Fang, W.-D., Tan, Q.-G., Ji, R., Yang, L.-Y., Wei, S., Zhang, X.-W., & Miao, A.-J. (2021). Photodegradation of carbon dots causes cytotoxicity. *Nature Communications, 12*(1), Article 812. https://doi.org/10.1038/s41467-021-21080-z

Louros, V. L., Ferreira, L. M., Silva, V. G., Silva, C. P., Martins, M. A., Otero, M., Esteves, V. I., & Lima, D. L. D. (2021). Photodegradation of aquaculture antibiotics using carbon dots–TiO_2 nanocomposites. *Toxics, 9*, Article 267. https://doi.org/10.3390/toxics9120330

Mahat, N. A., & Shamsudin, S. A. (2020). Blue luminescence carbon quantum dots derived from oil palm empty fruit bunch biomass. *IOP Conference Series: Materials Science and Engineering, 736*(5), Article 052001. https://doi.org/10.1088/1757-899X/736/5/052001

Mintz, K. J., Zhou, Y., & Leblanc, R. M. (2019). Recent development of carbon quantum dots regarding their optical properties, photoluminescence mechanism, and core structure. *Nanoscale, 11*(11), 4634-4652. https://doi.org/10.1039/C8NR10059D

Mukherjee, I., Cilamkoti, V., & Dutta, R. K. (2021). Sunlight-driven photocatalytic degradation of ciprofloxacin by carbon dots embedded in ZnO nanostructures. *ACS Applied Nano Materials, 4*(8), 7686-7697.https://doi.org/10.1021/acsanm.1c00883

Nair, S. S. P., Kottam, N., & Kumar S. G. P. (2020). Green synthesised luminescent carbon nanodots for the sensing application of Fe^{3+} ions. *Journal of Fluorescence, 30*(2), 357-363.https://doi.org/10.1007/s10895-020-02505-2 Niu, J., Ding, S., Zhang, L., Zhao, J., & Feng, C. (2013). Visible-light-mediated Sr-Bi_2O_3 photocatalysis of tetracycline: Kinetics, mechanisms and toxicity assessment. *Chemosphere, 93*(1), 1-8. https://doi.org/10.1016/j.chemosphere.2013.04.043

Pelaez, M., Nolan, N. T., Pillai, S. C., Seery, M. K., Falaras, P., Kontos, A. G., Dunlop, P. S. M., Hamilton, J. W. J., Byrne, J. A., O'Shea, K., Entezari, M. H., & Dionysiou, D. D. (2012). A review on the visible light active titanium dioxide photocatalysts for environmental applications. *Applied Catalysis B: Environmental, 125*, 331-349. https://doi.org/10.1016/j.apcatb.2012.05.036

Saadati, F., Keramati, N., & Ghazi, M. M. (2016). Influence of parameters on the photocatalytic degradation of tetracycline in wastewater: A review. *Critical Reviews in Environmental Science and Technology, 46*(8), 757-782. https://doi.org/10.1080/10643389.2016.1159093

Safari, G. H., Hoseini, M., Seyedsalehi, M., Kamani, H., Jaafari, J., & Mahvi, A. H. (2015). Photocatalytic degradation of tetracycline using nanosized titanium dioxide in aqueous solution. *International Journal of Environmental Science and Technology, 12*(2), 603-616. https://doi.org/10.1007/s13762-014-0706-9

Sahu, V., & Sahoo, S. K. (2024). Biogenic synthesis of carbon dots with inbuilt biological activity. *Next Nanotechnology, 5*, 100034. https://doi.org/10.1016/j.nxnano.2023.100034

Sawalha, S., Azzam, H., Bin Ali, R., Dweikat, H., & Anaya, K. (2021, October 12-14). Photodegradation of methylene blue by carbon nanodots synthesised from olive solid wastes [Conference paper]. *Proceedings of the 9th Jordan International Chemical Engineering Conference (JICHEC9), Jordan*.

Sharma, M., Mandal, M. K., Pandey, S., Kumar, R., & Dubey, K. K. (2022). Visible-light-driven photocatalytic degradation of tetracycline using heterostructured Cu_2O–TiO_2 nanotubes: Kinetics and toxicity evaluation of degraded products on cell lines. *ACS Omega, 7*(37), 33572-33586. https://doi.org/10.1021/acsomega.2c04576

Sharma, N., Sharma, I., & Bera, M. K. (2022). Microwave-assisted green synthesis of carbon quantum dots derived from *Calotropis gigantea* as a fluorescent probe for bioimaging. *Journal of Fluorescence, 32*(3), 1039-1049. https://doi.org/10.1007/s10895-022-02923-4

Sutanto, H., Alkian, I., Romanda, N., Lewa, I. W. L., Marhaendrajaya, I., & Triadyaksa, P. (2020). High green-emission carbon dots and its optical properties: Microwave power effect. *AIP Advances, 10*(5), Article 055013.https://doi.org/10.1063/5.0004595

Syahin, M., Zamri, F. A., & Sapawe, N. (2019). Kinetic study on photocatalytic degradation of phenol using green electrosynthesised TiO_2 nanoparticles. *Materials Today: Proceedings, 19*, 2214-2219.https://doi.org/10.1016/j.matpr.2019.11.131

Thiang, E. L., Lee, C. W., Takada, H., Seki, K., Takei, A., Suzuki, S., Wang, A., & Bong, C. W. (2021). Antibiotic residues from aquaculture farms and their ecological risks in Southeast Asia: A case study from Malaysia. *Ecosystem Health and Sustainability, 7*(1), Article 1926337. https://doi.org/10.1080/20964129.2021.1926337

Trenczek-Zając, A., Synowiec, M., Zakrzewska, K., Zazakowny, K., Kowalski, K., Dziedzic, A., & Radecka, M. (2022). Scavenger-supported photocatalytic evidence of an extended type I electronic structure of the TiO_2@Fe_2O_3 interface. *ACS Applied Materials & Interfaces, 14*(33), 38255-38269. https://doi.org/10.1021/acsami.2c06404

Ţucureanu, V., Matei, A., & Avram, A. M. (2016). FTIR spectroscopy for carbon family study. *Critical Reviews in Analytical Chemistry, 46*(6), 502-520. https://doi.org/10.1080/10408347.2016.1157013

Wang, W., Lemaire, R., Bensakhria, A., & Luart, D. (2022). Review on the catalytic effects of alkali and alkaline earth metals (AAEMs), including sodium, potassium, calcium and magnesium, on the pyrolysis of lignocellulosic biomass and on the co-pyrolysis of coal with biomass. *Journal of Analytical and Applied Pyrolysis, 163*, 105479. https://doi.org/10.1016/j.jaap.2022.105479

World Health Organisation. (2021). *Antimicrobial resistance*. https://www.who.int/groups/framework-development-stewardship-AMR

Wu, S., Hu, H., Lin, Y., Zhang, J., & Hu, Y. H. (2020a). Visible light photocatalytic degradation of tetracycline over TiO_2. *Chemical Engineering Journal, 382*, 122842. https://doi.org/10.1016/j.cej.2019.122842

Wu, S., Li, X., Tian, Y., Lin, Y., & Hu, Y. H. (2021b). Excellent photocatalytic degradation of tetracycline over black anatase-TiO_2 under visible light. *Chemical Engineering Journal, 406*, 126747.https://doi.org/10.1016/j.cej.2020.126747

Xu, J. J., Lu, Y. N., Tao, F. F., Liang, P. F., & Zhang, P. A. (2023). ZnO nanoparticles modified by carbon quantum dots for the photocatalytic removal of synthetic pigment pollutants. *ACS Omega, 8*(8), 7845-7857.https://doi.org/10.1021/acsomega.2c07591

Yan, M., Yan, Y., Wu, Y., Shi, W., & Hua, Y. (2015). Microwave-assisted synthesis of monoclinic-tetragonal $BiVO_4$ heterojunctions with enhanced visible-light-driven photocatalytic degradation of tetracycline. *RSC Advances, 5*(110), 90255-90264. https://doi.org/10.1039/C5RA13684A

Zhong, Q., Lin, Q., Huang, R., Fu, H., Zhang, X., Luo, H., & Xiao, R. (2020). Oxidative degradation of tetracycline using persulfate activated by N and Cu codoped biochar. *Chemical Engineering Journal, 380*, 122608.https://doi.org/10.1016/j.cej.2019.122608

Zhou, Y., Mintz, K. J., Oztan, C. Y., Hettiarachchi, S. D., Peng, Z., Seven, E. S., Liyanage, P. Y., De La Torre, S., Celik, E., & Leblanc, R. M. (2018). Embedding carbon dots in superabsorbent polymers for additive manufacturing. *Polymers, 10*(8), Article 921. https://doi.org/10.3390/polym10080921